JAM-C Is Important for Lens Epithelial Cell Proliferation and Lens Fiber Maturation in Murine Lens Development

Qihang Sun, Jiani Li, Jingyu Ma, Yuxing Zheng, Rong Ju, Xuri Li, Xiangrong Ren, Lijuan Huang, Rongyuan Chen, Xuhua Tan, and Lixia Luo

State Key Laboratory of Ophthalmology, Zhongshan Ophthalmic Center, Sun Yat-sen University, Guangdong Provincial Key Laboratory of Ophthalmology and Visual Science, Guangzhou, China

Correspondence: Lixia Luo, Jinsui Road No. 7, State Key Laboratory of Ophthalmology, Zhongshan Ophthalmic Center, Sun Yat-sen University, Guangdong Provincial Key Laboratory of Ophthalmology and Visual Science, Guangzhou 510060, China; luolixia@mail.sysu.edu.cn.
Xuhua Tan, Jinsui Road No. 7, State Key Laboratory of Ophthalmology, Zhongshan Ophthalmic Center, Sun Yat-sen University, Guangdong Provincial Key Laboratory of Ophthalmology and Visual Science, Guangzhou 510060, China; tanxh6@mail.sysu.edu.cn.
Rongyuan Chen, Jinsui Road No. 7, State Key Laboratory of Ophthalmology, Zhongshan Ophthalmic Center, Sun Yat-sen University, Guangdong Provincial Key Laboratory of Ophthalmology and Visual Science, Guangzhou 510060, China; nullall@163.com.

QS, JL, and JM contributed equally to this work.

Received: September 3, 2023
Accepted: November 16, 2023
Published: December 14, 2023

Citation: Sun Q, Li J, Ma J, et al. JAM-C is important for lens epithelial cell proliferation and lens fiber maturation in murine lens development. *Invest Ophthalmol Vis Sci.* 2023;64(15):15. https://doi.org/10.1167/iovs.64.15.15

Purpose. The underlying mechanism of congenital cataracts caused by deficiency or mutation of junctional adhesion molecule C (JAM-C) gene remains unclear. Our study aims to elucidate the abnormal developmental process in *Jamc*$^{-/-}$ lenses and reveal the genes related to lens development that JAM-C may regulate.

Methods. *Jamc* knockout (*Jamc*$^{-/-}$) mouse embryos and pups were generated for in vivo studies. Four key developmental stages from embryonic day (E) 12.5 to postnatal day (P) 0.5 were selected for the following experiments. Hematoxylin and eosin staining was used for histological analysis. The 5-bromo-2′-deoxyuridine (BrdU) incorporation assay and TUNEL staining were performed to label lens epithelial cell (LEC) proliferation and apoptosis, respectively. Immunofluorescence and Western blot were used to analyze the markers of lens epithelium, cell cycle exit, and lens fiber differentiation.

Results. JAM-C was expressed throughout the process of lens development. Deletion of *Jamc* resulted in decreased lens size and disorganized lens fibers, which arose from E16.5 and aggravated gradually. The LECs of *Jamc*$^{-/-}$ lenses showed decreased quantity and proliferation, accompanied with reduction of key transcription factor, FOXE3. The fibers in *Jamc*$^{-/-}$ lenses were disorganized. Moreover, *Jamc*-deficient lens fibers showed significantly altered distribution patterns of Cx46 and Cx50. The marker of fiber homeostasis, γ-crystallin, was also decreased in the inner cortex and core fibers of *Jamc*$^{-/-}$ lenses.

Conclusions. Deletion of JAM-C exhibits malfunction of LEC proliferation and fiber maturation during murine lens development, which may be related to the downregulation of FOXE3 expression and abnormal localization patterns of Cx46 and Cx50.

Keywords: JAM-C, lens development, cell proliferation, FOXE3 connexins

Mammalian lens development is a precisely regulated process. Taking the murine lens as an example, the lens ectoderm thickens to form the lens placode and invaginates to become the lens pit.[1] When the lens pit deepens and is separated from the ectoderm to form the lens vesicle, the cells on the anterior hemisphere differentiate into lens epithelium and the posterior cells elongate and differentiate into primary fibers that gradually fill the lumen of the lens vesicle, which occur at around E12.5.[2] At E13.5 to E14.5, as the apical side of primary fibers has reached the lens epithelium, the lens epithelial cells (LECs) start to divide and migrate to the transition zone,[3,4] where they differentiate into secondary fibers and add to the mass of primary fibers.[5] During the terminal differentiation stages, the lens fibers undergo a series of maturation processes to make the lens a highly transparent organ, including accumulation of crystallins and degradation of nuclei and organelles.[6] These processes are repeated throughout life and the latter one first begins at the late embryonic stage (after E16.5). Any dysregulation that occurs during the lens development process can lead to the loss of lens transparency, namely, congenital cataract.

Congenital cataract, defined as opacification of the lens at birth, is the leading cause of visual impairment in children worldwide.[7,8] Statistical analysis reported that about one quarter of congenital cataracts can be attributed to gene mutations.[9] The mutated genes related to congenital cataract can be divided into four types: genes encoding crystallins (*CRYAA*,[10] *CRYAB*,[11] *CRYGD*,[12] etc.), membrane proteins (*GJA3*,[13] *GJA8*,[14] *MIP*,[15] etc.), cytoskeletal components (*BFSP1*,[16] *BFSP2*,[17] *FYCO1*,[18] etc.) and transcription factors (*HSF4*,[19] *FOXE3*,[20] *PAX6*,[20] etc.).

Among the membrane proteins, JAM-C is a subtype of the JAM family, which belongs to type I transmembrane proteins with two extracellular immunoglobulin (Ig)-like domains, a single transmembrane-spanning domain, and a canonical PDZ domain-binding motif at the cytoplasmic tail.[21] JAM-C is widely localized at tight junctions of epithelial cells.[22] The homozygous mutation of *JAMC* genes in humans results in severe developmental defects, including congenital cataract, hemorrhagic destruction of the brain, and subependymal calcification.[23–25] Our recent study has reported that *Jamc*$^{-/-}$ mice exhibit congenital cataract, accompanied by abnormal activation of unfolded protein response (UPR) and increased fiber cell death in postnatal lenses.[26] These findings indicate that JAM-C plays a significant role in lens development. However, how JAM-C regulates lens development remains unclear.

In this study, we traced the changes in *Jamc*$^{-/-}$ lenses at different stages of embryonic development process and found that *Jamc*$^{-/-}$ lenses exhibiting smaller lens sizes and disrupted fiber organization start at E16.5. *Jamc*$^{-/-}$ lenses showed reduced LEC population and proliferation accompanied by decreased FOXE3 expression. Moreover, several abnormalities in the terminal differentiation of lens fiber cells (LFCs), including the significant alteration of the expression pattern of key gap junction proteins, Cx46 and Cx50, were also found in *Jamc*$^{-/-}$ lenses. Collectively, JAM-C maintains the proliferation of LEC, and maturation and homeostasis of LFC, which reveals its crucial role in lens development.

Materials and Methods

Animals

All animal experimental procedures were conducted in accordance with the ARVO Statement for the Use of Animals in Ophthalmic and Vision Research and were approved by the animal research ethics committee at the Zhongshan Ophthalmic Center, Sun Yat-sen University. The *Jamc* knockout mice strain, C57bL/6-Jam3$^{tm1.1Chav}$ (http://www.informatics.jax.org/allele/MGI:5140157), was a gift from Triantafyllos Chavakis, MD (Technische Universität Dresden, Saxony, Germany). The wild type strain refers to *Jamc*$^{+/+}$ mice and knockout (*Jamc*$^{-/-}$) mice were achieved by intercrossing *Jamc*$^{+/-}$ mice. Embryo ages were defined by the appearance of the vaginal plug (embryonic day 0.5 [E0.5]).

Hematoxylin and Eosin Staining and Immunofluorescence

Histological section, hematoxylin and eosin (H&E) staining and immunofluorescent staining were performed as in our previous report.[26] Briefly, for H&E staining, fresh eyeballs or embryonic heads were fixed in FAS Eyeball Fixative Solution (Servicebio, Wuhan, China) and embedded in paraffin. Then, the 5 µm-thick sagittal sections were cut through the midsection of the lens. For immunofluorescent staining, eyeballs or embryonic heads were fixed in 0.75% paraformaldehyde overnight at 4°C and then washed in PBS, followed by gradient dehydration in 10% to 30% sucrose, embedding in the optimal cutting temperature (OCT) compound (Crystalgen, Inc., Commack, NY, USA). Cryosections with a thickness of 10 µm were cut through the sagittal plane. Sections were air dried and received antigen retrieval by heating the slides in sodium citrate buffer. After blocking in 5% donkey serum for 30 minutes, the tissues were incubated with the following primary antibodies overnight at 4°C: goat anti-JAM-C (1:50, AF1213; R&D Systems), mouse anti-FOXE3 (1:200, sc-377465; Santa Cruz), mouse anti-BrdU (1:200, 5292S; Cell Signaling Technology), rabbit anti-ZO-1 (1:200, 40-2200; Invitrogen), rabbit anti-PAX6 (1:500, ab195045; Abcam), goat anti-PROX1 (1:200, AF2727; R&D Systems), rabbit anti-p27^{KIP1} (1:200, 3686; Cell Signaling Technology), mouse anti-p57^{KIP2} (1:100, sc-56341; Santa Cruz), rabbit anti-βB1-crystallin (1:200, ab232799; Abcam), mouse anti-γ-crystallin (1:200, sc-365256; Santa Cruz), mouse anti-Connexin 46 (1:200, sc-377398; Santa Cruz), and rabbit anti-Connexin 50 (1:200, ab222885; Abcam). Sections were then incubated with Alexa Fluor-conjugated secondary antibodies (1:500; Invitrogen) for 1 hour at room temperature and counterstained with 0.1% DAPI (1:1000, D8417; Sigma) for 10 minutes. For F-actin staining, sections without the antigen retrieval process were incubated with Alexa Fluor-conjugated phalloidin (1:200, A12379, Invitrogen) for 2 hours at room temperature. Images were acquired using a Zeiss Axio Imager.Z2 microscope, LSM710 or LSM980 confocal microscope (Carl Zeiss, Zena, Germany) and processed using the ZEN software (version 2.3; Carl Zeiss Microscopy, Germany).

5-Bromo-2′-Deoxyuridine Incorporation Assay

Pregnant mice or neonatal pups were injected intraperitoneally with 100 mg/kg of body weight of 5-bromo-2′-deoxyuridine (BrdU, B5002; Sigma). After 2 hours, the animals were euthanized and the embryos were dissected. Subsequent treatments were identical to the methods described in the Hematoxylin and Eosin Staining and Immunofluorescence section.

Protein Extraction and Western Blot

The protein extraction and immunoblot assay were performed as our previous methods.[26] In brief, 2 lenses from P0.5 neonatal mice were ground and lysed in radioimmunoprecipitation assay buffer containing protease and phosphatase inhibitor cocktails (A32961; Thermo Fisher Scientific). Samples were loaded 25 µg per lane separated on a 4% to 20% sodium dodecyl sulfate-polyacrylamide gel electrophoresis (SDS-PAGE) gel (ET12420Gel; ACE Biotechnology) and transferred to a polyvinylidene difluoride (PVDF) membrane (162-0177; Bio-Rad Laboratories, Hercules, CA, USA). After blocking with 5% non-fat milk, the membrane was incubated with primary antibodies overnight at 4°C, followed by incubation with horseradish peroxidase (HRP)-conjugated secondary antibodies (1:5000, Multi Sciences, Hangzhou, China) for 1 hour at room temperature. The Immobilon Western Chemiluminescent HRP substrate (MilliporeSigma, Burlington, MA, USA) was used to detect specific antibody binding. Signals were captured using a Syngene

G:BOX Chemi XT16 imaging device (Syngene, Cambridge, UK). Primary antibodies used are as follows: goat anti-JAM-C (1:500, AF1213; R&D Systems), rabbit anti-JAM-C (1:1000, 40-9000; Invitrogen), mouse anti-FOXE3 (1:250, sc-377465; Santa Cruz), mouse anti-α-tubulin (1:2000, RM2007; Beijing Ray Antibody Biotech), rabbit anti-PAX6 (1:1000, ab195045; Abcam), mouse anti-βB1-crystallin (1:200, sc-48335; Santa Cruz), mouse anti-γ-crystallin (1:200, sc-365256; Santa Cruz), mouse anti-Connexin 46 (1:1000, sc-377398; Santa Cruz), rabbit anti-Connexin 50 (1:1000, ab222885; Abcam), mouse anti-β-actin (1:2000, RM2001; Beijing Ray Antibody Biotech), and rabbit anti-HSP90 (1:3000, 13171-1-AP; Proteintech). The intensities of the bands were analyzed using the tool "Gels" in ImageJ software (National Institutes of Health [NIH], Bethesda, MD, USA) and normalized to loading control. Quantification was performed on lenses from three wild type and *Jamc*$^{-/-}$ mice.

TUNEL Staining

Free 3′-OH DNA double-strand ends were detected using the TUNEL BrightRed Apoptosis Detection Kit (A113-02; Vazyme) according to the manufacturer's protocol. Briefly, cryosections were digested with proteinase K, and then incubated in a TdT reaction mix for 1 hour at 37°C. Cell nuclei were stained with 0.1% DAPI (1:1000, D8417; Sigma). Sections were analyzed using a Zeiss LSM710 confocal microscope (Carl Zeiss, Zena, Germany).

Image Analysis

The colocalization analyses were conducted by ImageJ software. The corresponding grayscale intensities of JAM-C and ZO-1 fluorescence in the lenses were generated using the "Plot Profile" tool in ImageJ as reported.[27] The colocalization scatterplot was generated by the "Coloc2" plugin in ImageJ.[28] The diameter of the lenses was measured using the ZEN software. For the analysis of LECs, the monolayer of DAPI^{+} cells at the anterior of the lenses was counted as LECs. DAPI^{+}, BrdU^{+}, and FOXE3^{+} LECs were counted using the "Cell Counter" plugin in ImageJ.[29] Quantification was performed on at least five sections per lens from three wild type and *Jamc*$^{-/-}$ embryos or neonatal mice.

Statistical Analysis

All data were represented as means ± standard error of the mean (SEM). GraphPad Prism (version 8.2.1; La Jolla, CA, USA) software was used for statistical analysis. Unpaired *t*-test was used to compare the means between the two groups. All statistical tests were two-tailed. The P values < 0.05 were considered statistically significant.

Results

Spatial and Temporal Expression of JAM-C During Murine Lens Development

To determine the expression pattern of JAM-C during lens development, we focused on 4 consecutive stages of lens development, including embryonic stage E12.5, E14.5, E16.5, and postnatal stage P0.5. At E12.5, JAM-C was expressed in LECs and the elongating primary fibers and the strongest signal of expression was detected at the apical-apical interface (Figs. 1A–C). To E14.5, JAM-C expression was also found in secondary fibers (Figs. 1D–F). From E16.5 to P0.5, JAM-C maintained the same distribution pattern as before (Figs. 1G–L). Specifically, magnified images show that in the lens epithelium, JAM-C exhibited a similar distribution pattern as the tight junction protein ZO-1 which is enriched at the apical surface (Figs. 1G1–I2). However, JAM-C had more staining in the central fibers than ZO-1. These results indicate that from E12.5 to postnatal stages, JAM-C is expressed in LECs, partially colocalized with ZO-1 (Figs. 1M, 1N) and expressed in LFCs.

Jamc-Deficient Lenses Exhibit Morphological Abnormalities at Late Embryonic Stages

Our previous study found that all *Jamc* knockout mice developed congenital nuclear cataracts by P21.[26] To further investigate the role of JAM-C in the early stages of lens development and determine when lens dysplasia emerges due to *Jamc* deficiency, we generated global *Jamc* knockout mice as previously described.[26] The knockout efficiency of *Jamc* was validated by Western Blot (Supplementary Fig. S1A) and immunofluorescent staining (Supplementary Fig. S1B).

At four specific developmental stages that were identical to Figure 1, we conducted a comparative morphological analysis between *Jamc*$^{-/-}$ embryos and their wild type littermates. There were no significant morphological differences between *Jamc*$^{-/-}$ and wild type lenses at E12.5 and E14.5 (Figs. 2A–D). However, starting at E16.5, *Jamc*$^{-/-}$ lenses showed decreased volume, posterior shift of the bow region (Figs. 2E, 2F, 2E1–F3) and signs of disarrangement of the core fibers (Figs. 2E3, 2F3).

To further reveal more detailed information, the magnified images of the outer cortex, inner cortex, and core were analyzed according to previous reports.[30–32] In the outer cortex of the wild type lens, where the newly differentiated secondary fibers gradually migrated from the convex to the concave toward the interior of the lens (Figs. 2E1, 2I), whereas in the *Jamc*$^{-/-}$ lens, this process seemed to be slowed down (Figs. 2F1, 2J). Furthermore, the posterior tips of newly differentiated fibers in the outer cortex of *Jamc*$^{-/-}$ lens appeared to be swollen, manifested by the dilation of cytoplasm (Figs. 2E4, 2F4, arrow heads). The fibers of the inner cortex of the wild type lens have all shown a concave direction toward the center (Fig. 2E2), whereas the fiber orientations in the same area of the *Jamc*$^{-/-}$ lens were obviously different as the directions of the fibers close to the core became disordered (Fig. 2F2). It is worth noting that the core region of the *Jamc*$^{-/-}$ lens was significantly moved anteriorly and was located closer to the epithelium rather than in the center of the lens like the wild type group (Fig. 2E3). The posterior suture also became significantly longer (Figs. 2E, 2F, 2E5, 2F5), and the fiber arrangement of the core was also disordered, as if they had been pushed or squeezed (Fig. 2F3). These developmental abnormalities were significantly exacerbated by P0.5 (Figs. 2G, 2H, 2G1–H5), with the central fibers exhibiting disarrangement and failed denucleation (Figs. 2G3, 2H3).

For a clearer view of the structure of fibers, we used phalloidin to label the actin cytoskeleton in the lenses. Consistent with the results of H&E staining, no significant abnormality was found in *Jamc*$^{-/-}$ lenses at E12.5 and E14.5

Investigative Ophthalmology & Visual Science

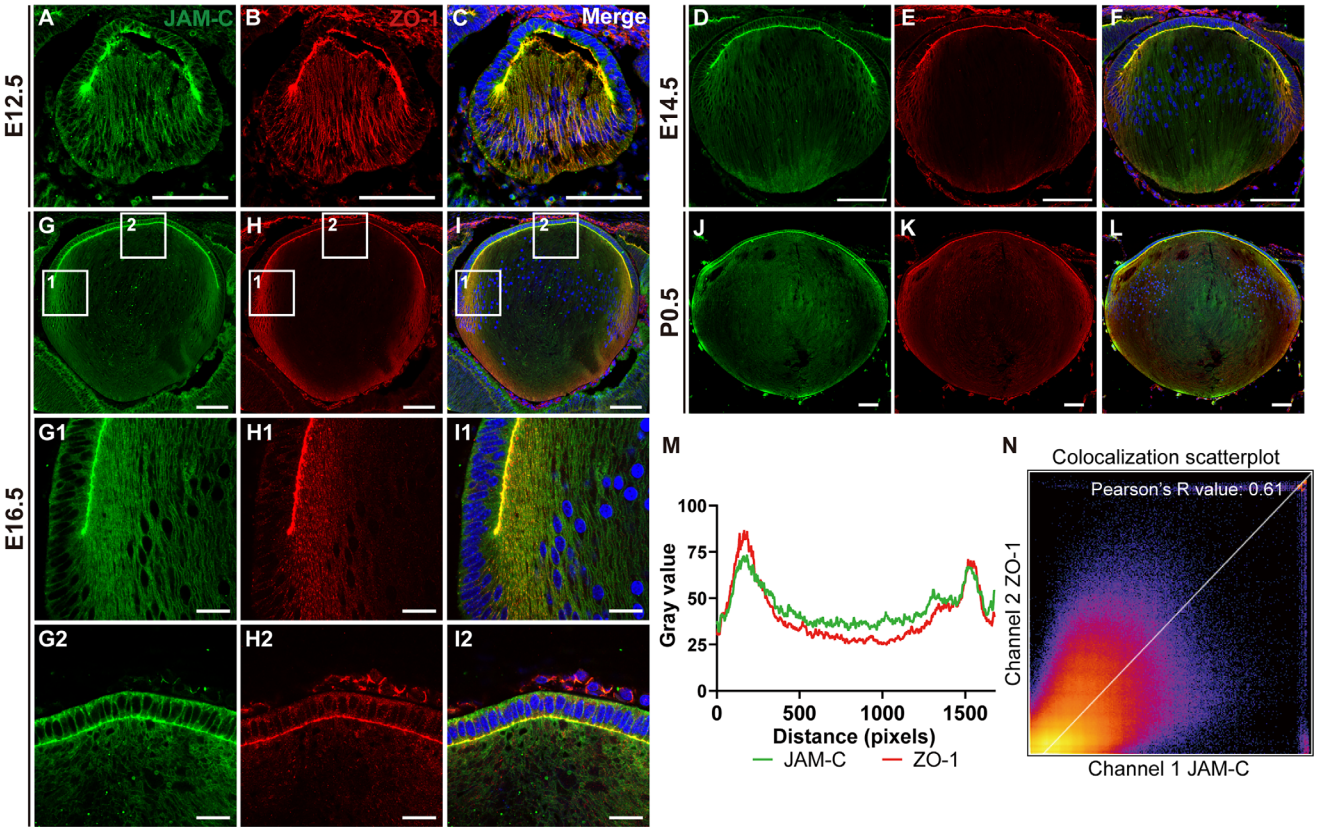

Figure 1. Expression and localization of JAM-C in lens developmental process. (**A–L**) Detection of JAM-C at four representative developmental stages. Immunofluorescence staining showed that JAM-C (*green*) is expressed throughout the lens developmental stages and overlaps with ZO-1 (*red*). Nuclei were counterstained with DAPI (*blue*). Scale bars = 100 µm. (**G1-I2**) Magnified images corresponding to the *white boxes* in **G** to **I** showed the localization of JAM-C in the lens epithelium and fibers. Scale bars = 20 µm. (**M**) Colocalization analysis generated by ImageJ. The signal of JAM-C is overlapped with ZO-1. (**N**) The colocalization scatter plot performed by the coloc2 plugin in ImageJ. The signal of JAM-C and ZO-1 has correlation (Pearson correlation coefficient > 0.5), which indicates that JAM-C colocalizes with ZO-1.

(Supplementary Figs. S2A–D). The changes in the outer cortex and the inner cortex at E16.5 and P0.5 were the same as those of H&E staining (Figs. 3A–D3). The fibers in the core region of *Jamc*$^{-/-}$ lenses even showed obvious signs of being compressed, with the cytoskeleton arranged like coil springs (Figs. 3A4, 3B4, 3C4, 3D4).

Taken together, deletion of *Jamc* may not affect lens morphogenesis in the early embryonic stage, but it results in suppressed lens growth, incorrect fiber orientation, and defects in core fibers in later developmental stages.

Decreased LEC Number and Proliferation in *Jamc*$^{-/-}$ Lenses

To further characterize the microphakia phenotype of *Jamc*$^{-/-}$ lenses, we measured the diameter of the lenses at different developmental stages. The sizes of *Jamc*$^{-/-}$ lenses were significantly smaller at E16.5 (Fig. 4A). Because the lens increases rapidly in volume from late developmental stages, which is associated with continued LEC proliferation, we hypothesized that JAM-C maintains LEC proliferation and regulates lens volume growth. First, we counted the number of LECs at different developmental stages and found that the number of LECs in *Jamc*$^{-/-}$ lenses was significantly less than that in wild type lenses at E16.5 (Fig. 4B), which was consistent with the trend of lens volume reduction. Next, we analyzed LECs in the proliferative state with BrdU. At E12.5 and E14.5, the proportion of proliferating LECs in the *Jamc*$^{-/-}$ lens was not significantly different from wild type (Figs. 4C, 4D1–G2). However, at E16.5, the LEC proliferation level of *Jamc*$^{-/-}$ lenses was significantly reduced (Figs. 4C, 4H1–I2).

To confirm that the reduced LEC number was due to decreased proliferation rather than increased apoptosis, we performed TUNEL assay and found no significant difference in LEC apoptosis levels between *Jamc*$^{-/-}$lenses and wild type group from E16.5 to P7 (Supplementary Figs. S3A–F). However, at P0.5, elevated apoptosis levels were found in the core region of *Jamc*$^{-/-}$ lenses (Figs. 4L–M1). At P7, more apoptotic fiber cells appeared in the inner cortex and core of the *Jamc*$^{-/-}$ lenses (Figs. 4O–P1), which was consistent with our previous report.[26] These results suggested that a decrease in lens volume due to *Jamc* knockout is associated with reduced LEC proliferation.

Loss of *Jamc* DownRegulates FOXE3 Expression in LEC Through a PAX6 Independent Manner

Forkhead box protein E3 (FOXE3), a key transcription factor involved in lens development, is expressed in the lens epithelium[33] and is considered to be essential for LEC proliferation.[34] We used immunofluorescence staining to

Investigative Ophthalmology & Visual Science

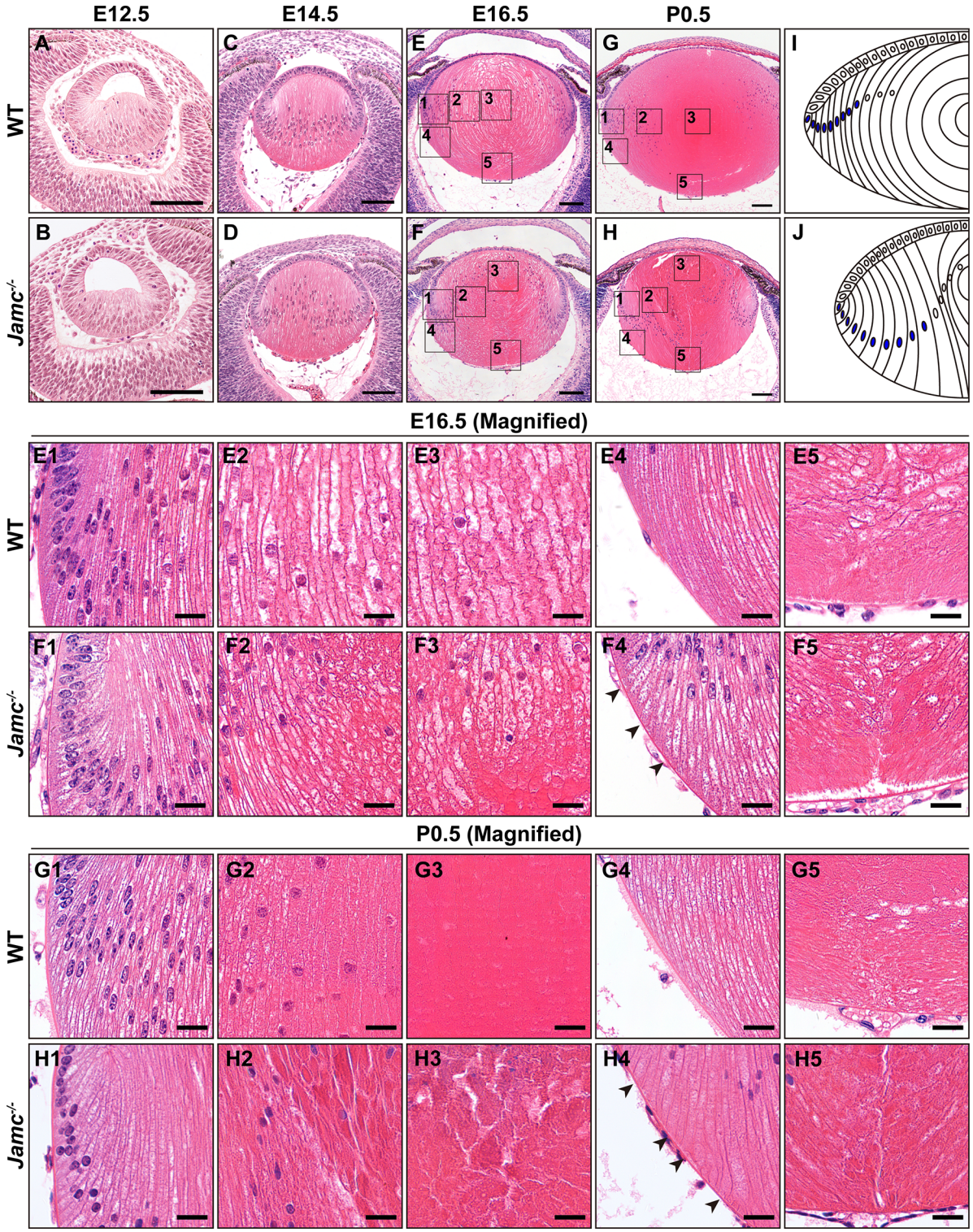

Figure 2. ***Jamc*$^{-/-}$ lenses exhibited morphological abnormalities in later embryonic 14 stages.** (**A–H**) H&E staining of wild type and *Jamc*$^{-/-}$ lenses at four representative developmental stages. Morphological defects of *Jamc*$^{-/-}$ lenses occurred at E16.5 and aggravated at P0.5. Scale bars = 100 µm. (**E1–H5**) Magnified images corresponding to the black boxes in **E** to **H**, showing the structures of the outer cortex (**E1**, **F1**, **G1**, and **H1**), inner cortex (**E2**, **F2**, **G2**, and **H2**), core (**E3**, **F3**, **G3**, and **H3**), posterior tips of fibers in the outer cortex (**E4**, **F4**, **G4**, and **H4**), and posterior sutures (**E5**, **F5**, **G5**, and **H5**). Scale bars = 20 µm. (**I, J**) Schematic diagram of incorrect orientation of secondary fibers and posterior displacement of the bow region (*blue* nuclei) in *Jamc*$^{-/-}$ lenses compared with wild type.

Investigative Ophthalmology & Visual Science

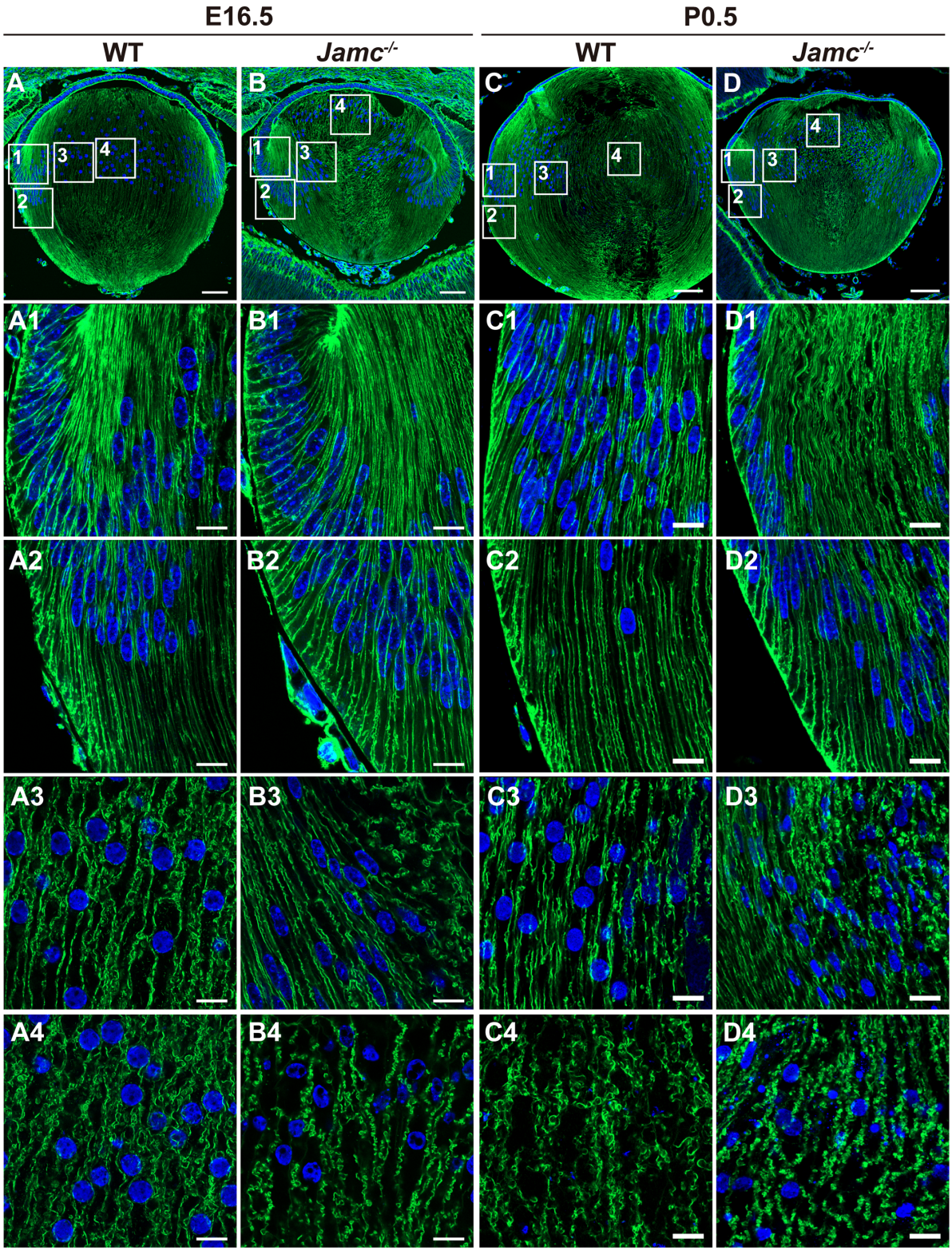

Figure 3. Cytoskeleton disorder in *Jamc*$^{-/-}$ fibers at later developmental stages. (**A–D**) F-actin cytoskeleton labeled by phalloidin (*green*) in wild type and *Jamc*$^{-/-}$ lenses at E16.5 and P0.5. Nuclei were counterstained with DAPI (*blue*). Scale bars = 100 µm. (**A1–D4**) Magnified images corresponding to the *white boxes* in **A** to **D**, showing the structures of the outer cortex (**A1**, **B1**, **C1**, and **D1**), posterior tips of the outer cortex fibers (**A2**, **B2**, **C2**, and **D2**), inner cortex (**A3**, **B3**, **C3**, and **D3**), and core (**A4**, **B4**, **C4**, and **D4**). Scale bars = 10 µm.

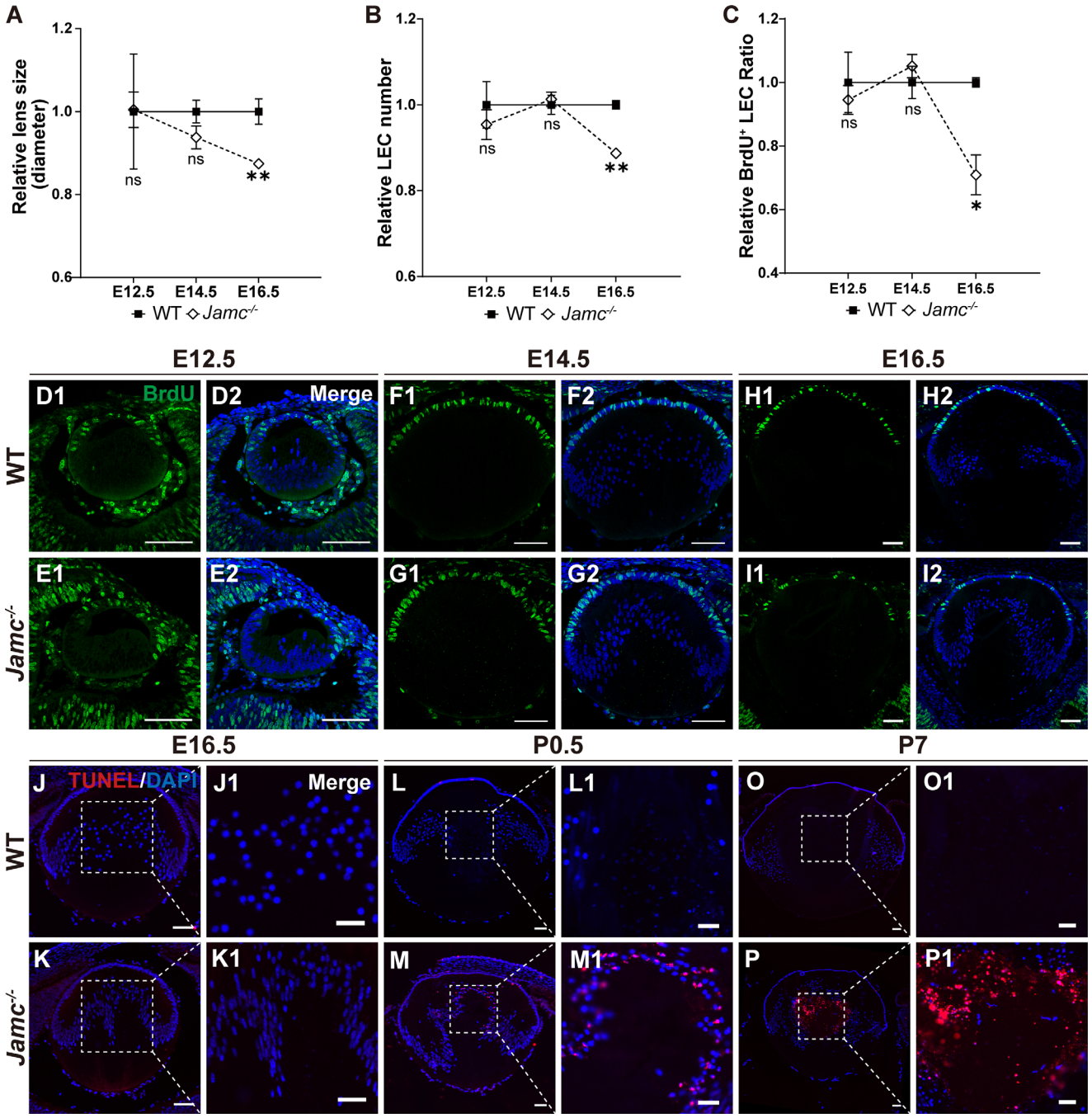

Figure 4. ***Jamc*$^{-/-}$ lenses showed smaller sizes and decreased LEC proliferation.** (**A**, **B**) Quantification of lens diameter and LEC number in wild type and *Jamc*$^{-/-}$ lenses from E12.5 to 16.5. Lens diameter was measured using the ZEN software. The monolayer of DAPI^{+} cells at the anterior of the lenses was counted as LECs. (**C**) Quantification of BrdU^{+} LECs (calculated as the ratio of BrdU/DAPI) in wild type and *Jamc*$^{-/-}$ lenses from E12.5 to 16.5 corresponding to D1 to I2. The BrdU^{+} and DAPI^{+} LECs were counted using the Cell Counter plugin in ImageJ software. *$P < 0.05$, **$P < 0.01$; $n = 3$. ns, not significant. (**D1–I2**) Immunofluorescence staining of BrdU (*green*) to label the S-phase of actively proliferating LECs. Nuclei were counterstained with DAPI (*blue*). The LECs labeled by BrdU significantly decreased in *Jamc*$^{-/-}$ lenses at E16.5. Scale bars = 100 µm. (**J–P1**) Representative immunofluorescent images of TUNEL (*red*) staining in wild type and *Jamc*$^{-/-}$ lenses at E16.5, P0.5, and P7. Nuclei were counterstained with DAPI (*blue*). **J1**, **K1**, **L1**, **M1**, **O1**, and **P1** are magnified images of the inner cortex and core fibers. Scale bars (**J–P**) = 100 µm. (**J1–P1**) scale bars = 50 µm.

detect the expression of FOXE3 at different stages of lens development. At E12.5 and E14.5, as with wild type lenses, FOXE3 of *Jamc*$^{-/-}$ lenses was localized in the nuclei of LECs and there was no significant difference in the proportion of FOXE3^{+} LECs between wild type and *Jamc*$^{-/-}$ lenses (Figs. 5A1–D2, I). However, by E16.5, there was a significant reduction in LECs expressing FOXE3 in *Jamc*$^{-/-}$ lenses (Figs. 5E1–F3, I). At P0.5, the proportion of FOXE3^{+} LECs in

Investigative Ophthalmology & Visual Science

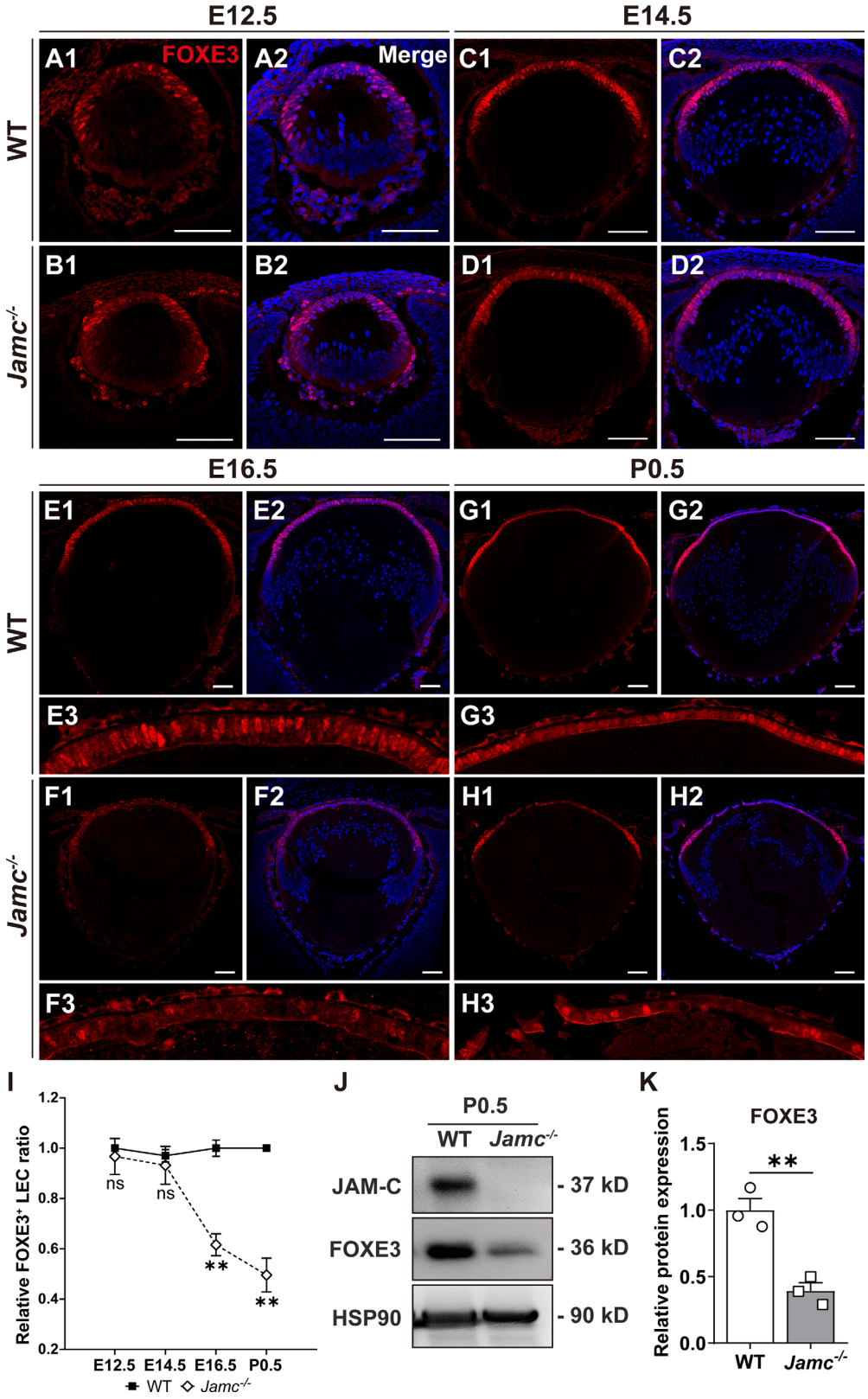

Figure 5. Decreased FOXE3 expression in *Jamc*$^{-/-}$ LECs during late developmental stages. (**A1–H3**) Immunofluorescence staining of FOXE3 (*red*) in wild type and *Jamc*$^{-/-}$ lenses. Nuclei were counterstained with DAPI (*blue*). FOXE3 is highly expressed in almost all LECs in wild type lenses and decreased in *Jamc*$^{-/-}$ lenses at E16.5 and P0.5. Scale bars = 100 µm. (**E3**, **F3**, **G3**, and **H3**) Magnified images of the LECs corresponding to **E1**, **F1**, **G1**, and **H1**. (**I**) Quantification of FOXE3^{+} LECs (calculated as the ratio of FOXE3^{+} to DAPI^{+} cells) in wild type and *Jamc*$^{-/-}$ lenses from E12.5 to P0.5 corresponding to **A1–H3**. The FOXE3^{+} and DAPI^{+} LECs were counted using the Cell Counter plugin in ImageJ software. $^{**}P < 0.01$; $n = 3$. (**J**) Immunoblot analysis of lens protein at P0.5 showed significantly decreased FOXE3 expression in *Jamc*$^{-/-}$ lenses. HSP90 was used as loading control. (**K**) Quantification of FOXE3 protein levels in **J**. $^{**}P < 0.01$; $n = 3$.

Investigative Ophthalmology & Visual Science

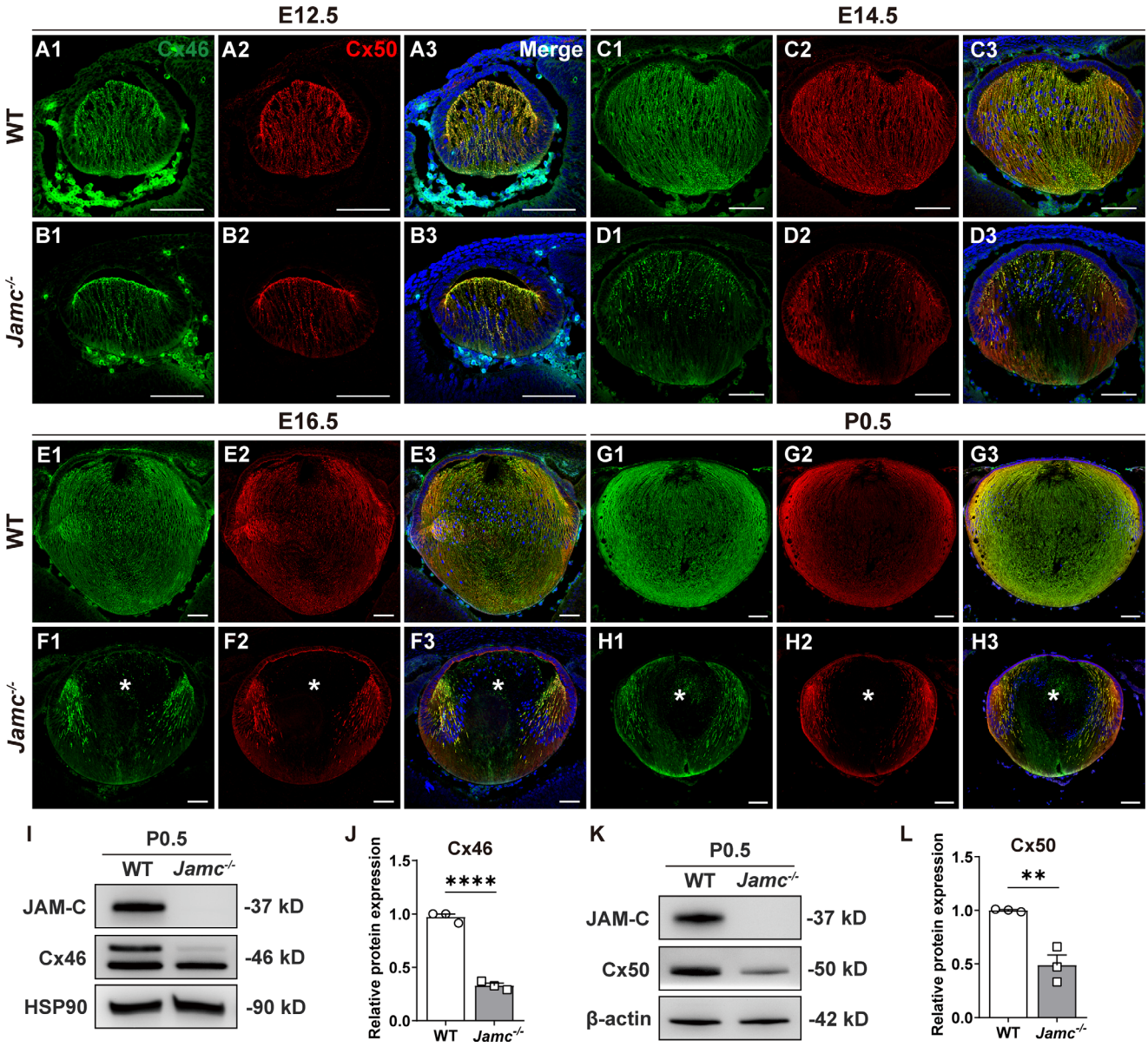

Figure 6. Disrupted expression and distribution of Cx46 and Cx50 in *Jamc*$^{-/-}$ lenses. (**A1–H3**) Representative immunofluorescent images of Cx46 (*green*) and Cx50 (*red*) in wild type and *Jamc*$^{-/-}$ lenses. Nuclei were counterstained with DAPI (*b*lue). The * symbols in **F1** to **F3** and **H1** to **H3** indicate the absence of Cx46 or Cx50 in the inner cortex and core fibers in *Jamc*$^{-/-}$ lenses. Scale bars = 100 µm. (**I**, **K**) Immunoblot analysis of lens protein at P0.5 showed significantly decreased Cx46 and Cx50 expression in *Jamc*$^{-/-}$ lenses. β-actin was used as loading control. (**J**, **L**) Quantification of Cx46 (upper band) and Cx50 protein levels in **I** and **K**. $^{**}P < 0.01$; $^{****}P < 0.0001$; $n = 3$.

the *Jamc*$^{-/-}$ lens decreased further, and Western Blot also confirmed a downregulation in protein levels (Figs. 5G1–H3, I–K). Moreover, the trend of FOXE3 reduction in the lens was consistent with the trend of LEC proliferation levels (see Figs. 4C–I2). Because PAX6 is an upstream regulator of FOXE3,[35] we wanted to know whether the reduction in FOXE3 due to *Jamc* knockout is related to PAX6. Immunofluorescence staining and Western Blot found that there was no significant difference in the expression and localization of PAX6 in *Jamc*$^{-/-}$ lenses and wild type lenses (Supplementary Fig. S5). These results suggested that *Jamc* deficiency leads to smaller lenses in mice may be partly due to the downregulation of FOXE3 in LEC without affecting PAX6 expression.

Cell Cycle Regulators in Differentiating Fibers are Largely Unchanged in *Jamc*$^{-/-}$ Lenses

Because *Jamc*$^{-/-}$ lenses showed a posterior shift of the transition zone and incorrect orientation of secondary fibers (see Figs. 2E–J), suggesting that the differentiation process into secondary fibers might be abnormal. During lens development, LECs exit the cell cycle in the transition zone and differentiate into secondary fibers.[3] In this process, PROX1 controls the expression of the cyclin kinase inhibitors p27^{Kip1} and p57^{Kip2},[36,37] which play an indispensable role. In our findings, the expression of PROX1 and p27^{Kip1} and p57^{Kip2} was specifically expressed in the nuclei of the transition zone in wild type lenses (Supplementary Figs. S6A–E,

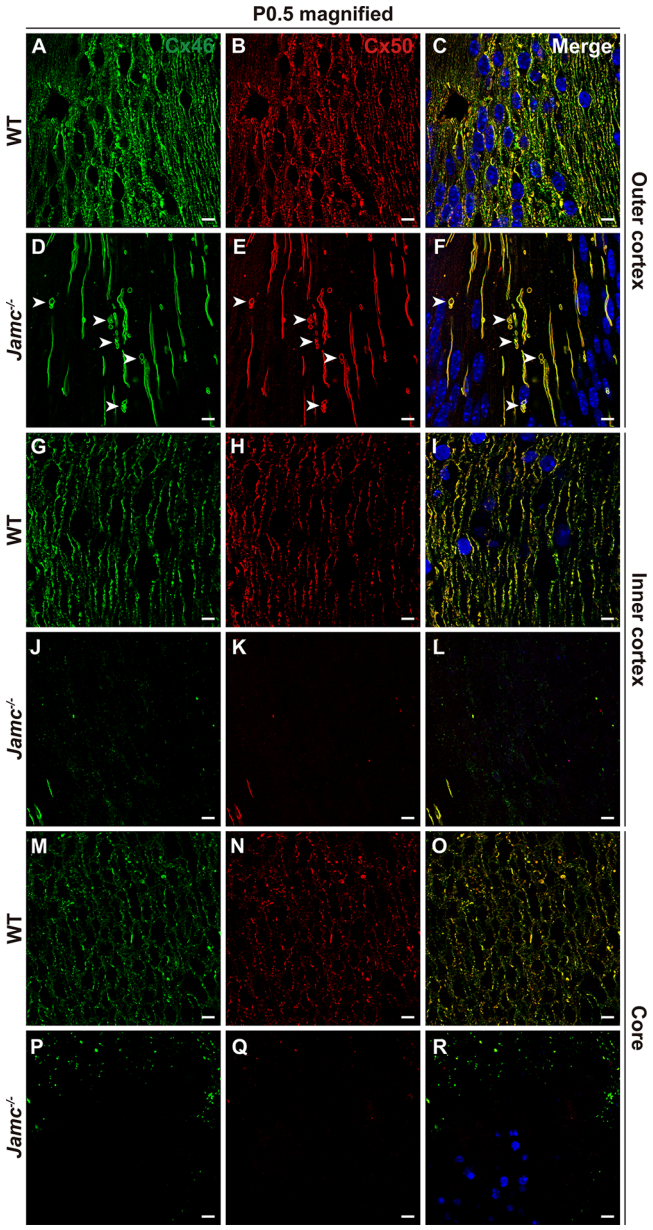

Figure 7. The different distribution pattern of Cx46 and Cx50 between wild type and *Jamc*$^{-/-}$ lenses. (**A–R**) Magnified immunofluorescent images of Cx46 (*green*) and Cx50 (*red*) in the outer cortex (**A–F**), inner cortex (**G–L**), and core (**M–R**) fibers of wild type and *Jamc*$^{-/-}$ lenses at P0.5. Nuclei were counterstained with DAPI (*blue*). Arrow heads in **D** to **F** are used to mark the vesicle-like structures in *Jamc*$^{-/-}$ lenses. Scale bars = 10 µm.

K–O). None of these three factors in *Jamc*$^{-/-}$ lenses changed significantly in expression and localization (Supplementary Figs. S6F–J, P–T). These results suggest that *Jamc* knockdown does not affect cell cycle exit during lens fiber differentiation.

Disrupted Expression of Connexins in *Jamc*$^{-/-}$ Lens Fibers During Lens Development

Gap junctions are abundantly expressed in lens fibers, including Cx46 and Cx50, play an important role in maintaining the homeostasis of the lens, especially the mature fibers located in the inner cortex and core.[38–40] Lenses with mutations or deletions of Cx46 and Cx50 showed swelling and deformation of inner fibers, failure of nuclear degradation, and congenital nuclear cataract,[41–44] which were extremely similar to the phenotype in *Jamc*$^{-/-}$ lenses. Therefore, we wondered whether there are abnormalities of Cx46/50 in *Jamc*$^{-/-}$ lens fibers. Immunofluorescent staining showed that from E12.5 to P0.5, Cx46 and Cx50 were expressed in wild type lens fibers (Figs. 6A1–A3, C1–C3, E1–E3, G1–G3). However, a completely different distribution pattern was shown in *Jamc*$^{-/-}$ lenses. At E12.5 and E14.5, both Cx46 and Cx50 densities were decreased in *Jamc*$^{-/-}$ lens fibers (Figs. 6B1–B3, D1–D3). At E16.5 to P0.5, the changes were more dramatic, with a sharp decrease of Cx46/50 staining in the inner fibers (Figs. 6F1–F3, H1–H3). The protein expression at P0.5 showed that both Cx46 and Cx50 in *Jamc*$^{-/-}$ lenses were significantly reduced (Figs. 6I–L). Magnified images of P0.5 showed that the regular distribution patterns of Cx46 and Cx50 in the outer cortex (Figs. 7A–C) were disrupted in the *Jamc*$^{-/-}$ lenses, which became longer lines with uneven distribution (Figs. 7D–F). In addition, several vesicle-like stainings were discovered in both wild type and *Jamc*$^{-/-}$ fibers, whereas the vesicle-like structures in *Jamc*$^{-/-}$ lenses were larger than those in wild type lenses (arrow heads in Figs. 7D–F). Cx46 and Cx50 were almost absent in the inner cortex and core of *Jamc*$^{-/-}$ lenses (Figs. 7J–L, P–R). Cx46 was largely colocalized with Cx50 in both wild type and *Jamc*$^{-/-}$ lens fibers. To show the relationship of connexins to the cell membrane, we used DiI to visualize the lipid membrane structures. Consistent with wild type group (see Supplementary Figs. S7A–C, G–I), the linear and vesicle-like structures of connexins in *Jamc*$^{-/-}$ fibers were colocalized with the lipid membrane (Supplementary Fig. S7D–F, J–L, arrow heads). It is speculated that these vesicle-like structures are intracellular vesicles that transport connexin to the cell membrane and that this transport process is abnormal in *Jamc*$^{-/-}$ fibers. These results suggested that the loss of *Jamc* leads to abnormal distribution of connexins in lens fibers, which may account for the disordered fiber arrangement and maturation.

Decrease in γ-Crystallin in *Jamc*$^{-/-}$ Lenses

The β-crystallin and γ-crystallin, which account for the majority of crystallin in the lens, are exclusively expressed in differentiated and mature lens fibers.[45,46] Mutations in the genes encoding any of them lead to cataract development.[47] Because *Jamc*$^{-/-}$ lenses showed disarrangement of central fibers and failure of denucleation, suggesting abnormal terminal differentiation and destruction of mature fiber homeostasis. We therefore wondered whether there were changes in β-crystallin and γ-crystallin in *Jamc*$^{-/-}$ lenses. Neither the localization nor the fluorescence intensity of these two types of crystallins appeared to change significantly in *Jamc*$^{-/-}$ lenses (Figs. 8A, B, D, E, Supplementary Fig. S8). Western Blot results at P0.5 showed unchanged β-crystallin level in *Jamc*$^{-/-}$ lenses while the protein level of γ-crystallin in *Jamc*$^{-/-}$ lenses was slightly reduced compared with wild type (Figs. 8G, H). Further analysis at P7 revealed that γ-crystallin staining in *Jamc*$^{-/-}$ lenses began to decrease in the inner cortex and significantly decreased in the core (dashed circles in Fig. 8F). The protein expression of γ-crystallin also decreased at P7 (Figs. 8I, J). These results indicated that the absence of *Jamc* disrupted the homeosta-

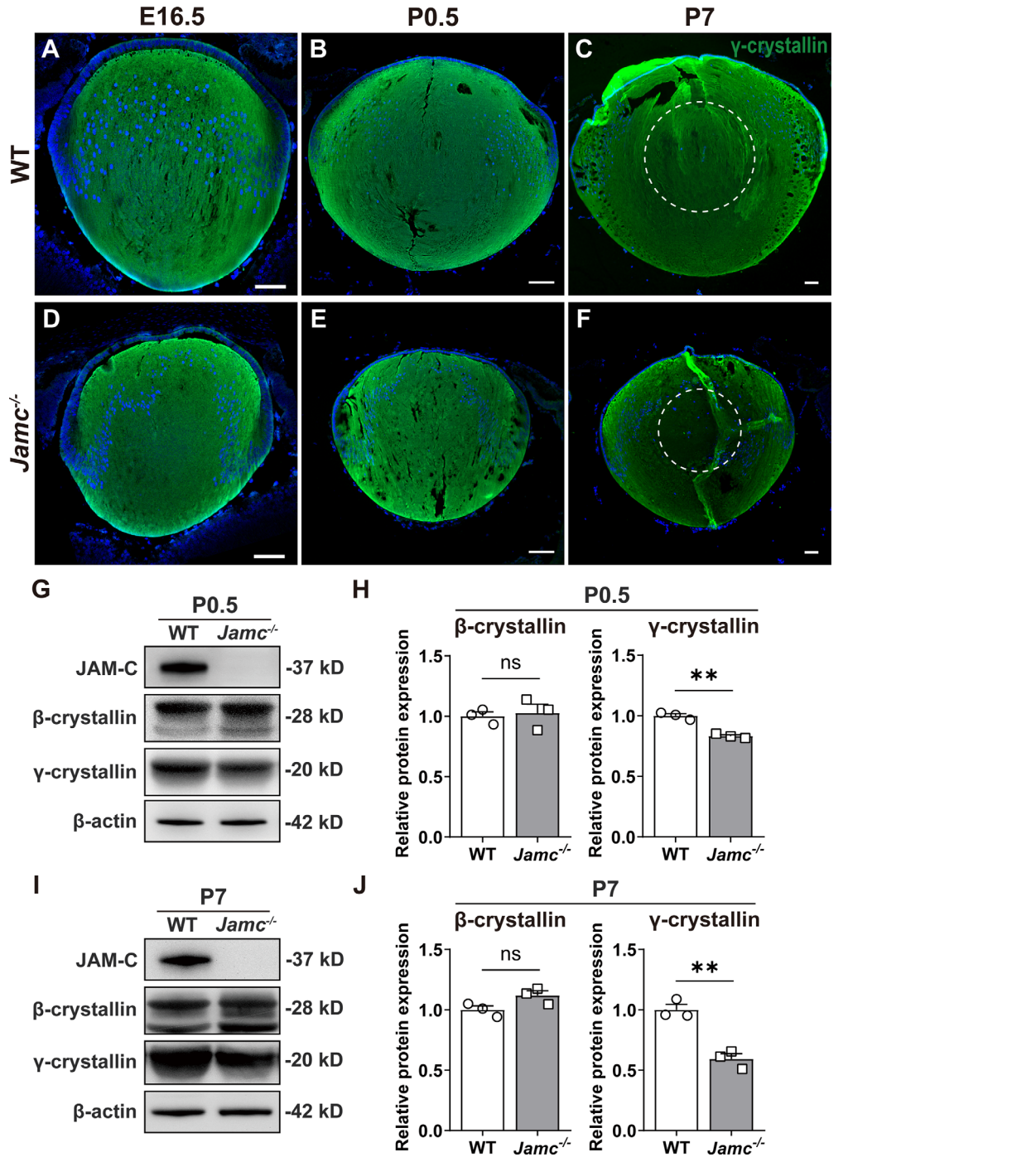

Figure 8. The expression and distribution of β- and γ-crystallin in *Jamc*$^{-/-}$ lenses. (**A–F**) Representative immunofluorescent images of γ-crystallin (*green*) in wild type and *Jamc*$^{-/-}$ lenses at E16.5, P0.5, and P7. Nuclei were counterstained with DAPI (*blue*). The inner cortex and core fibers (marked by *dashed circle*) of *Jamc*$^{-/-}$ lenses at P7 showed less γ-crystallin staining than wild type group. Scale bars = 100 µm. (**G**, **I**) Immunoblot analysis of lens proteins of wild type and *Jamc*$^{-/-}$ lenses at P0.5 and P7. The β-actin was used as loading control. (**H**, **J**) Quantification of β-crystallin and γ-crystallin protein levels in **G** and **I**. *Jamc*$^{-/-}$ lenses showed a slight decrease in γ-crystallin expression at P0.5, a significant decrease in γ-crystallin expression at P7 and no changes in β-crystallin expression. $^{**}P < 0.01$; $n = 3$.

sis of mature lens fibers, characterized by the reduction of γ-crystallin rather than β-crystallin.

Discussion

JAM-C is a subtype of junctional adhesion molecules, which is mainly located at the tight junctions of epithelial or endothelial cells and plays an important role in regulating cell polarity, migration, and differentiation.[21] Studies have found that JAM-C is expressed in the retina, promoting normal retinal development, stratification, and maturation of photoreceptors.[22,48] A membrane proteomic analysis revealed that JAM-C is expressed in the mouse lens fibers.[49] Mutation of *JAMC* gene results in congenital cataract

in humans.[23–25] Our recent study has reported the congenital nuclear cataract phenotype in *Jamc*$^{-/-}$ mice.[26] These findings indicate that JAM-C plays a significant role in lens development and drive us to explore how JAM-C regulates and maintains normal lens development. Our results identified two major roles of JAM-C in murine lens development: (1) maintaining normal proliferation of LECs, and (2) promoting fiber maturation.

The expression pattern of JAM-C in developing murine lens showed high expression at the apical surface of the lens epithelium, which colocalized with ZO-1. Moreover, JAM-C exhibited a clear expression in lens fibers whereas tight junctions have not been reported to exist in lens fiber compartment,[49] indicating that JAM-C may play a role in lens fibers other than tight junctions. Knockout of *Jamc* resulted in decreased lens size and disorganized lens fibers at E16.5. The fiber cells in the outer cortex of the *Jamc*$^{-/-}$ lenses showed incorrect orientation and swelling posterior tips. With the lengthened posterior suture and absent anterior suture, the core was shifted anteriorly and was compressed and distorted. It can be speculated that the deficiency of *Jamc* caused the newly differentiated fibers in the outer cortex to be misoriented and the posterior tips to be swollen, resulting in the contact of the posterior tips happening earlier than the anterior tips of the fibers to form the posterior suture, thereby squeezing the primary fibers in the core toward the front. This eventually led to front-to-back asymmetry, failure of anterior suture formation, and disorganized core fibers. These histological defects suggest that JAM-C plays a crucial role in murine lens development, especially in late embryonic stages. Moreover, we noticed that *Jamc*$^{-/-}$ retinas showed thinner outer nuclear layer (ONL) and thicker ganglion cell layer (GCL) at P0.5 (data not shown), which is consistent with a previous report at 2 months old.[50] Considering that the interaction between retina and lens in the early developmental stage is critical to lens morphogenesis, the indirect effect of JAM-C on lens development by influencing the retina cannot be ignored.

A significant abnormality of *Jamc*$^{-/-}$ lenses is microphakia. Because the consistent proliferation and differentiation of LECs contribute to the rapid growth of lens size during the late embryonic and early postnatal stages,[4] we hypothesized that *Jamc* knockout may disturb the proliferation of LECs. Intriguingly, the proliferation level of LECs in *Jamc*$^{-/-}$ lenses decreased at E16.5, which is consistent with reduced LEC numbers at the same stage. These suggested that JAM-C is essential for lens epithelial proliferation. The role of tight junction proteins in regulating cell proliferation has been widely reported.[51] Mutated JAM-C protein inhibits the proliferation and migration of lung carcinoma cell lines.[52] Treatment with anti-JAM-C antibody significantly decreased the proliferation of JAM-C-expressing lymphoma B cells in vitro, probably through inhibiting the phosphorylation of ERK1/2.[53] Our study provided in vivo evidence that JAM-C maintains normal LEC proliferation during lens development. Further studies will focus on exploring the underlying signaling pathways involved in this process such as RTKs.[54]

FOXE3, a member of the forkhead box family, is a key transcription factor in lens development. It is expressed in the lens placode at E9.5 and later restricted to the lens epithelium.[33] FOXE3 is considered to be essential for lens epithelial proliferation and the closure of the lens vesicle.[34] Mutations in the human *FOXE3* gene are commonly associated with microphthalmia, aphakia, and glaucoma.[55,56] *Foxe3* knockout mice exhibit abnormal lens development, including microphakia, decreased LEC proliferation, and premature fiber differentiation.[33] It has been reported that FOXE3 expression can be regulated by other transcription factors, such as PAX6.[35] However, the regulatory network of FOXE3 in lens development is largely unknown. Our data discovered that the downregulation of FOXE3 in the *Jamc*$^{-/-}$ lenses occurred in the central epithelium. The decrease of FOXE3 made them lose the LEC identity, whereas the FOXE3 expression in the LECs close to the transition zone in *Jamc*$^{-/-}$ lenses was not affected. In addition, we found that the trend of FOXE3 reduction was consistent with that of reduced LEC proliferation. Therefore, we speculate that the reduction of FOXE3 caused by *Jamc* knockout may be one of the reasons for the retarded proliferation of LEC. We speculate that JAM-C may be a potential regulator of FOXE3 during lens development. However, there are still some issues to be clarified. Once the lens epithelium becomes abnormal, the lens fibers from which they differentiate will subsequently be involved, thus partially explaining the later onset of the phenotype. However, considering the early expression of JAMC and FOXE3, and the crucial role FOXE3 plays in early lens morphogenesis, an earlier phenotype should commence if JAM-C is indeed an upstream of FOXE3. However, the downregulation of FOXE3 followed by *Jamc* knockout was only observed in the later stages of embryonic development, suggesting that certain specific events may happen during such a later stage. Therefore, whether there is a connection between JAM-C and FOXE3 needs further verification and the exact regulating mechanism remains to be unveiled in the future.

Due to *Jamc* knockout, the newly differentiated secondary fibers in the outer cortex appeared misoriented and the transition zone shifted backward, suggesting an abnormal differentiation process. An important hallmark of lens fiber differentiation is cell cycle exit, which is mediated by the transcription factor PROX1[37] and its downstream cell cycle-dependent kinase inhibitors $p27^{KIP1}$ and $p57^{KIP2}$.[57,58] These proteins are highly expressed in the transition zone and hardly expressed in LECs. *Jamc* deficiency did not alter the region-specific expression of PROX1, $p27^{KIP1}$, and $p57^{KIP2}$ in the developing lens. This suggests that JAM-C may not be involved in regulating cell cycle exit during lens fiber differentiation, which could also explain why the newly differentiated fibers of *Jamc*$^{-/-}$ lens did not show severe defects. JAM-C may regulate the orientation and migration of early lens fibers through other pathways.

The most significant defect of *Jamc*$^{-/-}$ lenses is the disarrangement of the inner cortex and core fibers. This characteristic phenotype drew our attention to the protein connexin, which maintains the homeostasis of mature lens fibers. During lens development, gap junctions are highly expressed in differentiated fibers, especially the mature fibers located in the interior. The gap junctions in the lens include Cx43, Cx46, and Cx50,[39] mainly the latter 2 in the fibers,[59,60] which assemble into channels on the cell membrane.[61] These channels provide pathways for intercellular and intracellular exchange of ions, small metabolites, and second messengers, such as $Ca2^{+}$, glutathione, and cAMP.[62,63] Any dysfunction of the channels will cause an imbalance of the internal homeostasis of the lens and lead to opacification. Mutations in genes encoding Cx46 and Cx50 lead to disrupted lens development and congenital cataracts in both humans and mice.[13,14,42–44] Moreover, markers of UPR and endoplasmic reticulum (ER) stress, including CHOP

and BiP, were detected in lens fibers of several Cx50 mice with different mutations,[64,65] with similarities to our previous findings in *Jamc*$^{-/-}$ lenses.[26] However, the fact that UPR caused by Cx50 mutations may be related to the failure of the mutated protein to transport to the cell membrane, thus accumulating in the ER. The expression of Cx46 and Cx50 in *Jamc*$^{-/-}$ lenses was downregulated and even missing in the inner cortex and core fibers, suggesting that the UPR caused by *Jamc* deficiency and the UPR caused by Cx50 mutation may not share the same mechanism. Notably, the compressed and disorganized fibers were located at the location where Cx46 and Cx50 were absent. The time at which these fibers begin to appear abnormal is observed in later developmental stages, and it is possible that fluid circulation of the lens is established at this time. Therefore, it is speculated that the possible mechanism is related to the function of connexin itself: connexin dysfunction leads to an imbalance of Ca^{2+} in lens fibers, which results in UPR and ER stress.[66] Taken together, our study reveals that JAM-C is required for the correct distribution of connexins during lens development and may maintain the maturation and homeostasis of lens fibers in this way. How JAM-C interacts with Cx46 and Cx50 remains unknown, but some speculation can be made based on large vesicle-like structures in fibers of the outer cortex. JAM-C may be required for Cx46/50 trafficking and proper assembly onto the cell membrane because connexins are transported in the form of intracellular vesicles and assembled onto the plasma membrane.[67,68] Our future studies will focus on the mechanism through which JAM-C interacts with connexins and regulates their functions.

In lens fibers, crystallins are the major cytoplasmic proteins that are involved in maintaining the refractive properties of the lens. Any factor that disrupts the homeostasis of lens fibers will affect their expression levels, solubility, or modified forms, resulting in lens opacification. Among them, β-crystallin and γ-crystallin accumulate in fiber cells and are molecular markers of lens fiber differentiation.[45,46] Furthermore, mouse models of cataracts with Cx46 or Cx50 deletion or mutation showed alterations in crystallins,[42,43,69,70] primarily γ-crystallin. However, all abnormalities of γ-crystallin appeared 14 to 21 days after birth, or even later. The expression of γ-crystallin in *Jamc*$^{-/-}$ lenses was slightly decreased at birth and significantly decreased at P7, suggesting that the disrupted homeostasis of mature lens fibers caused by *Jamc* deficiency was aggravated at postnatal stages. It is unclear how the absence of *Jamc* leads to a decrease in γ-crystallin level during the differentiation and maturation of lens fibers, it may relate to the dysregulation of connexins or the destruction of the membrane-cytoskeleton structures of the mature fibers in the inner cortex and core.

In summary, JAM-C is required for normal LEC proliferation and fiber maturation during murine lens development. *Jamc*-deficiency resulted in smaller lens size at E16.5 due to reduced LEC proliferation. Loss of *Jamc* disrupted the correct orientation of newly differentiated secondary fibers in the outer cortex; the inner cortex and core fibers failed to mature and became disordered. Besides, the expression of connexins, which play an important role in maintaining the homeostasis of mature lens fibers, was downregulated. These factors jointly lead to the destruction of the homeostasis of mature fiber in the inner cortex and core, with the reduction of γ-crystallin expression, which finally manifested as the formation of congenital cataract. Still, potential stress resulted from retinal defects in *Jamc* global knockout eyes cannot be excluded, the specific roles of JAM-C in lens development remain to be defined using genetic tools to interfere JAM-C expression in lens epithelium. In conclusion, the findings of this article expand our understanding of lens development and provide new insights into the pathogenesis of congenital cataract.

Acknowledgments

The authors thank the staff of Laboratory Animal Center and Core Facilities at State Key Laboratory of Ophthalmology, Zhongshan Ophthalmic Center for technical support.

Supported by the National Natural Science Foundation of China (Nos. 82070940 and 82070941).

Disclosure: **Q. Sun**, None; **J. Li**, None; **J. Ma**, None; **Y. Zheng**, None; **R. Ju**, None; **X. Li**, None; **X. Ren**, None; **L. Huang**, None; **R. Chen**, None; **X. Tan**, None; **L. Luo**, None

References

1. McAvoy JW. Cytoplasmic processes interconnect lens placode and optic vesicle during eye morphogenesis. *Exp Eye Res*. 1980;31:527–534.
2. Coulombre JL, Coulombre AJ. Lens development: fiber elongation and lens orientation. *Science*. 1963;142:1489–1490.
3. Griep AE. Cell cycle regulation in the developing lens. *Semin Cell Dev Biol*. 2006;17:686–697.
4. Cvekl A, Ashery-Padan R. The cellular and molecular mechanisms of vertebrate lens development. *Development*. 2014;141:4432–4447.
5. Lovicu FJ, McAvoy JW. Growth factor regulation of lens development. *Dev Biol*. 2005;280:1–14.
6. Brennan L, Disatham J, Kantorow M. Mechanisms of organelle elimination for lens development and differentiation. *Exp Eye Res*. 2021;209:108682.
7. Foster A, Gilbert C, Rahi J. Epidemiology of cataract in childhood: a global perspective. *J Cataract Refract Surg*. 1997;23(Suppl 1):601–604.
8. Khokhar SK, Pillay G, Dhull C, Agarwal E, Mahabir M, Aggarwal P. Pediatric cataract. *Indian J Ophthalmol*. 2017;65:1340–1349.
9. Li J, Chen X, Yan Y, Yao K. Molecular genetics of congenital cataracts. *Exp Eye Res*. 2020;191:107872.
10. Hansen L, Yao W, Eiberg H, et al. Genetic heterogeneity in microcornea-cataract: five novel mutations in CRYAA, CRYGD, and GJA8. *Invest Ophthalmol Vis Sci*. 2007;48:3937–3944.
11. Jiao X, Khan SY, Irum B, et al. Missense mutations in CRYAB are liable for recessive congenital cataracts. *PLoS One*. 2015;10:e0137973.
12. Mackay DS, Bennett TM, Culican SM, Shiels A. Exome sequencing identifies novel and recurrent mutations in GJA8 and CRYGD associated with inherited cataract. *Hum Genomics*. 2014;8:19.
13. Berry V, Ionides ACW, Pontikos N, et al. Whole-genome sequencing reveals a recurrent missense mutation in the Connexin 46 (GJA3) gene causing autosomal-dominant lamellar cataract. *Eye (Lond)*. 2018;32:1661–1668.
14. Ceroni F, Aguilera-Garcia D, Chassaing N, et al. New GJA8 variants and phenotypes highlight its critical role in a broad spectrum of eye anomalies. *Hum Genet*. 2019;138:1027–1042.
15. Senthil Kumar G, Kyle JW, Minogue PJ, et al. An MIP/AQP0 mutation with impaired trafficking and function underlies an autosomal dominant congenital lamellar cataract. *Exp Eye Res*. 2013;110:136–141.

16. Ramachandran RD, Perumalsamy V, Hejtmancik JF. Autosomal recessive juvenile onset cataract associated with mutation in BFSP1. *Hum Genet*. 2007;121:475–482.
17. Conley YP, Erturk D, Keverline A, et al. A juvenile-onset, progressive cataract locus on chromosome 3q21-q22 is associated with a missense mutation in the beaded filament structural protein-2. *Am J Hum Genet*. 2000;66:1426–1431.
18. Chen J, Ma Z, Jiao X, et al. Mutations in FYCO1 cause autosomal-recessive congenital cataracts. *Am J Hum Genet*. 2011;88:827–838.
19. Bu L, Jin Y, Shi Y, et al. Mutant DNA-binding domain of HSF4 is associated with autosomal dominant lamellar and Marner cataract. *Nat Genet*. 2002;31:276–278.
20. Brémond-Gignac D, Bitoun P, Reis LM, Copin H, Murray JC, Semina EV. Identification of dominant FOXE3 and PAX6 mutations in patients with congenital cataract and aniridia. *Mol Vis*. 2010;16:1705–1711.
21. Ebnet K. Junctional adhesion molecules (JAMs): cell adhesion receptors with pleiotropic functions in cell physiology and development. *Physiol Rev*. 2017;97:1529–1554.
22. Economopoulou M, Hammer J, Wang F, Fariss R, Maminishkis A, Miller SS. Expression, localization, and function of junctional adhesion molecule-C (JAM-C) in human retinal pigment epithelium. *Invest Ophthalmol Vis Sci*. 2009;50:1454–1463.
23. Mochida GH, Ganesh VS, Felie JM, et al. A homozygous mutation in the tight-junction protein JAM3 causes hemorrhagic destruction of the brain, subependymal calcification, and congenital cataracts. *Am J Hum Genet*. 2010;87:882–889.
24. De Rose DU, Gallini F, Battaglia DI, et al. A novel homozygous variant in JAM3 gene causing hemorrhagic destruction of the brain, subependymal calcification, and congenital cataracts (HDBSCC) with neonatal onset. *Neurol Sci*. 2021;42:4759–4765.
25. Akawi NA, Canpolat FE, White SM, et al. Delineation of the clinical, molecular and cellular aspects of novel JAM3 mutations underlying the autosomal recessive hemorrhagic destruction of the brain, subependymal calcification, and congenital cataracts. *Hum Mutat*. 2013;34:498–505.
26. Li J, Tan X, Sun Q, Li X, Chen R, Luo L. Deficiency of jamc leads to congenital nuclear cataract and activates the unfolded protein response in mouse lenses. *Invest Ophthalmol Vis Sci*. 2022;63:1.
27. Tisi A, Carozza G, Leuti A, Maccarone R, Maccarrone M. Dysregulation of resolvin E1 metabolism and signaling in a light-damage model of age-related macular degeneration. *Int J Mol Sci*. 2023;24:6749.
28. Rajani S, Gell C, Abakir A, Markus R. Computational analysis of DNA modifications in confocal images. *Methods Mol Biol*. 2021;2198:227–254.
29. Costa S, Schutz S, Cornec D, et al. B-cell and T-cell quantification in minor salivary glands in primary Sjögren's syndrome: development and validation of a pixel-based digital procedure. *Arthritis Res Ther*. 2016;18:21.
30. Li L, Lim J, Jacobs MD, Kistler J, Donaldson PJ. Regional differences in cystine accumulation point to a sutural delivery pathway to the lens core. *Invest Ophthalmol Vis Sci*. 2007;48:1253–1260.
31. Lim J, Li L, Jacobs MD, Kistler J, Donaldson PJ. Mapping of glutathione and its precursor amino acids reveals a role for GLYT2 in glycine uptake in the lens core. *Invest Ophthalmol Vis Sci*. 2007;48:5142–5151.
32. Nakazawa Y, Donaldson PJ, Petrova RS. Verification and spatial mapping of TRPV1 and TRPV4 expression in the embryonic and adult mouse lens. *Exp Eye Res*. 2019;186:107707.
33. Medina-Martinez O, Brownell I, Amaya-Manzanares F, Hu Q, Behringer RR, Jamrich M. Severe defects in proliferation and differentiation of lens cells in Foxe3 null mice. *Mol Cell Biol*. 2005;25:8854–8863.
34. Blixt A, Mahlapuu M, Aitola M, Pelto-Huikko M, Enerbäck S, Carlsson P. A forkhead gene, FoxE3, is essential for lens epithelial proliferation and closure of the lens vesicle. *Genes Dev*. 2000;14:245–254.
35. Dimanlig PV, Faber SC, Auerbach W, Makarenkova HP, Lang RA. The upstream ectoderm enhancer in Pax6 has an important role in lens induction. *Development*. 2001;128:4415–4424.
36. Zhao H, Yang T, Madakashira BP, et al. Fibroblast growth factor receptor signaling is essential for lens fiber cell differentiation. *Dev Biol*. 2008;318:276–288.
37. Wigle JT, Chowdhury K, Gruss P, Oliver G. Prox1 function is crucial for mouse lens-fibre elongation. *Nat Genet*. 1999;21:318–322.
38. Shi Y, Li X, Yang J. Mutations of CX46/CX50 and cataract development. *Front Mol Biosci*. 2022;9:842399.
39. Quan Y, Du Y, Tong Y, Gu S, Jiang JX. Connexin gap junctions and hemichannels in modulating lens redox homeostasis and oxidative stress in cataractogenesis. *Antioxidants (Basel)*. 2021;10:1374.
40. Mathias RT, White TW, Gong X. Lens gap junctions in growth, differentiation, and homeostasis. *Physiol Rev*. 2010;90:179–206.
41. Xia C-H, Liu H, Cheung D, et al. Diverse gap junctions modulate distinct mechanisms for fiber cell formation during lens development and cataractogenesis. *Development*. 2006;133:2033–2040.
42. Xia C-h, Cheng C, Huang Q, et al. Absence of alpha3 (Cx46) and alpha8 (Cx50) connexins leads to cataracts by affecting lens inner fiber cells. *Exp Eye Res*. 2006;83:688–696.
43. Gong X, Li E, Klier G, et al. Disruption of alpha3 connexin gene leads to proteolysis and cataractogenesis in mice. *Cell*. 1997;91:833–843.
44. Rong P, Wang X, Niesman I, et al. Disruption of Gja8 (alpha8 connexin) in mice leads to microphthalmia associated with retardation of lens growth and lens fiber maturation. *Development*. 2002;129:167–174.
45. Hejtmancik JF, Wingfield PT, Sergeev YV. Beta-crystallin association. *Exp Eye Res*. 2004;79:377–383.
46. Wang K, Cheng C, Li L, et al. GammaD-crystallin associated protein aggregation and lens fiber cell denucleation. *Invest Ophthalmol Vis Sci*. 2007;48:3719–3728.
47. Graw J. Genetics of crystallins: cataract and beyond. *Exp Eye Res*. 2009;88:173–189.
48. Daniele LL, Adams RH, Durante DE, Pugh EN, Philp NJ. Novel distribution of junctional adhesion molecule-C in the neural retina and retinal pigment epithelium. *J Comp Neurol*. 2007;505:166–176.
49. Bassnett S, Wilmarth PA, David LL. The membrane proteome of the mouse lens fiber cell. *Mol Vis*. 2009;15:2448–2463.
50. Li Y, Zhang F, Lu W, Li X. Neuronal expression of junctional adhesion molecule-C is essential for retinal thickness and photoreceptor survival. *Curr Mol Med*. 2018;17:497–508.
51. Díaz-Coránguez M, Liu X, Antonetti DA. Tight junctions in cell proliferation. *Int J Mol Sci*. 2019;20:5972.
52. Garrido-Urbani S, Vonlaufen A, Stalin J, et al. Junctional adhesion molecule C (JAM-C) dimerization aids cancer cell migration and metastasis. *Biochim Biophys Acta Mol Cell Res*. 2018;1865:638–649.
53. Doñate C, Vijaya Kumar A, Imhof BA, Matthes T. Anti-JAM-C therapy eliminates tumor engraftment in a xenograft model of mantle cell lymphoma. *J Leukoc Biol*. 2016;100:843–853.
54. Cvekl A, Zhang X. Signaling and gene regulatory networks in mammalian lens development. *Trends Genet*. 2017;33:677–702.

Investigative Ophthalmology & Visual Science

55. Anand D, Agrawal SA, Slavotinek A, Lachke SA. Mutation update of transcription factor genes FOXE3, HSF4, MAF, and PITX3 causing cataracts and other developmental ocular defects. *Hum Mutat*. 2018;39:471–494.
56. Semina EV, Brownell I, Mintz-Hittner HA, Murray JC, Jamrich M. Mutations in the human forkhead transcription factor FOXE3 associated with anterior segment ocular dysgenesis and cataracts. *Hum Mol Genet*. 2001;10:231–236.
57. Zhang P, Wong C, DePinho RA, Harper JW, Elledge SJ. Cooperation between the Cdk inhibitors p27(KIP1) and p57(KIP2) in the control of tissue growth and development. *Genes Dev*. 1998;12:3162–3167.
58. Zhang P, Liégeois NJ, Wong C, et al. Altered cell differentiation and proliferation in mice lacking p57KIP2 indicates a role in Beckwith-Wiedemann syndrome. *Nature*. 1997;387:151–158.
59. Paul DL, Ebihara L, Takemoto LJ, Swenson KI, Goodenough DA. Connexin46, a novel lens gap junction protein, induces voltage-gated currents in nonjunctional plasma membrane of Xenopus oocytes. *J Cell Biol*. 1991;115:1077–1089.
60. White TW, Bruzzone R, Goodenough DA, Paul DL. Mouse Cx50, a functional member of the connexin family of gap junction proteins, is the lens fiber protein MP70. *Mol Biol Cell*. 1992;3:711–720.
61. Jiang JX, Goodenough DA. Heteromeric connexons in lens gap junction channels. *Proc Natl Acad Sci USA*. 1996; 93:1287–1291.
62. Saez JC, Berthoud VM, Branes MC, Martinez AD, Beyer EC. Plasma membrane channels formed by connexins: their regulation and functions. *Physiol Rev*. 2003;83:1359–1400.
63. Harris AL. Emerging issues of connexin channels: biophysics fills the gap. *Q Rev Biophys*. 2001;34:325–472.
64. Berthoud VM, Minogue PJ, Lambert PA, Snabb JI, Beyer EC. The cataract-linked mutant connexin50D47A causes endoplasmic reticulum stress in mouse lenses. *J Biol Chem*. 2016;291:17569–17578.
65. Alapure BV, Stull JK, Firtina Z, Duncan MK. The unfolded protein response is activated in connexin 50 mutant mouse lenses. *Exp Eye Res*. 2012;102:28–37.
66. Bahar E, Kim H, Yoon H. ER stress-mediated signaling: action potential and Ca(2+) as key players. *Int J Mol Sci*. 2016;17:1558.
67. Totland MZ, Rasmussen NL, Knudsen LM, Leithe E. Regulation of gap junction intercellular communication by connexin ubiquitination: physiological and pathophysiological implications. *Cell Mol Life Sci*. 2020;77:573–591.
68. Laird DW, Naus CC, Lampe PD. SnapShot: connexins and disease. *Cell*. 2017;170:1260.
69. Berthoud VM, Minogue PJ, Yu H, Schroeder R, Snabb JI, Beyer EC. Connexin50D47A decreases levels of fiber cell connexins and impairs lens fiber cell differentiation. *Invest Ophthalmol Vis Sci*. 2013;54:7614–7622.
70. White TW, Goodenough DA, Paul DL. Targeted ablation of connexin50 in mice results in microphthalmia and zonular pulverulent cataracts. *J Cell Biol*. 1998;143:815–825.

Investigative Ophthalmology & Visual Science